OsRAD21-3, an orthologue of yeast *RAD21,* is required for pollen development in *Oryza sativa*

Jiayi Tao[1,2,3], Liangran Zhang[1,2,†], Kang Chong[1,2] and Tai Wang[1,2,*]

[1]*Research Center for Molecular and Developmental Biology, Key Laboratory of Photosynthesis and Environmental Molecular Physiology, Institute of Botany, Chinese Academy of Sciences, 20 Nanxincun, Xiangshan, Haidianqu, Beijing 100093, China,*
[2]*The National Center for Plant Gene Research, Beijing 100093, China, and*
[3]*Graduate School of Chinese Academy of Sciences, Beijing 100049, China*

Summary

In contrast to animals, in which products of meiosis differentiate directly into sperm, flowering plants employ a specific mechanism to give rise to functional sperm cells, the specifics of which remain largely unknown. A previous study revealed that, compared to yeast and vertebrates, which have two proteins (Rad21 and its meiosis-specific variant Rec8) that play a vital role in sister chromatid cohesion and segregation for mitosis and meiosis, respectively, the rice genome encodes four Rad21/Rec8 proteins (OsRad21s). In this paper, phylogenetic and immunostaining analyses reveal that OsRad21-3 is an orthologue of yeast Rad21. *OsRAD21-3* transcript and protein accumulated preferentially in flowers, with low levels in vegetative tissues. In flowers, they persisted from the stamen and carpel primordia stages until the mature pollen stage. OsRAD21-3-deficient RNAi lines showed arrested pollen mitosis, aberrant pollen chromosome segregation and aborted pollen grains, which led to disrupted pollen viability. However, male meiosis in these RNAi lines did not appear to be severely disrupted, which suggests that the main involvement of *OsRAD21-3* is in post-meiotic pollen development by affecting pollen mitosis. Furthermore, of the four *OsRAD21* genes in the rice genome, only *OsRAD21-3* was expressed in pollen grains. Given that the mechanism involving generation of sperm cells differs between flowering plants and metozoans, this study shows, in part, why flowering plants of rice and Arabidopsis have four Rad21/Rec8 proteins, as compared with two in yeast and metozoans, and gives some clues to the functional differentiation of Rad21/Rec8 proteins during evolution.

Keywords: *Oryza sativa*, OsRad21-3, Rad21, pollen mitosis, pollen development.

Introduction

In flowering plants, the highly specialized haploid male gametophyte (pollen) that is generated from diploid pollen mother cells (PMCs) in anthers is a key regulator of sexual reproduction and contributes to the genetic diversity of a population. The formation of pollen involves two principal phases: microsporogenesis and microgametogenesis. During microsporogenesis, PMCs are differentiated from archesporial cells, and thereafter undergo meiosis to generate haploid microspores. During microgametogenesis, the microspore released from tetrads quickly increases in size and then undergoes asymmetric mitosis (pollen mitosis I, PMI) to yield a large vegetative cell and a small generative cell. The large vegetative cell exits the cell cycle, and contains a dispersed nucleus and most of the cytoplasm from the microspore, whereas the diminutive generative cell has a condensed nucleus and a small amount of cytoplasm, and undergoes a second mitosis (pollen mitosis II, PMII), generating two sperm cells (McCormick, 2004; Twell, 2002; Wilson and Yang, 2004). In some plants, the second mitosis occurs in the growing pollen tube, whereas in other species, such as grasses and crucifers, it is completed before anthesis (Ma, 2005; McCormick, 2004). In contrast to the formation of germ cells in animals (Wilson and Yang, 2004), the two cycles of

mitosis at the post-meiotic stage are specific to flowering plants.

Recent efforts to decipher molecular events underlying male meiosis have extended our understanding of pollen development, in particular genetic studies, which have identified a number of meiotic mutants in *Arabidopsis thaliana*, *Zea mays* and *Oryza sativa* (Ma, 2005). Furthermore, forward and reverse genetic studies have functionally identified some key genes involved in male meiosis, including those involved in homologue pairing, recombination, repair and sister chromatid cohesion in these plants (Ma, 2005). In contrast, although some mutants involved in male mitosis have been identified in Arabidopsis (Chen and McCormick, 1996; Durbarry et al., 2005; Iwakawa et al., 2006; Lalanne et al., 2004; McCormick, 2004; Park et al., 1998; Twell, 2002), our knowledge of the mechanism underlying male mitosis is still limited.

Meiosis and mitosis involve a series of events, including sister chromatid cohesion, that are coordinated in time to guarantee faithful segregation of chromosomes. The cohesion binds newly replicated sister chromatids from S phase until the metaphase–anaphase transition, and is mediated by a phylogenetically conserved multi-protein cohesin complex (Lee and Orr-Weaver, 2001; Nasmyth, 2001). Mitotic cohesion in *Schizosaccharomyces pombe* and *Saccharomyces cerevisiae* involves at least Rad21 (also called Scc1 or Mcd1), Scc3, Smc1 and Smc3, and Rad21 is a vital subunit of the complex (Guacci et al., 1997; Michaelis et al., 1997). At the metaphase–anaphase transition, proteolytic cleavage of Rad21 mediated by separase triggers dissociation of cohesion proteins from chromosomes. The cleavage is necessary and sufficient for sister separation (Tomonaga et al., 2000; Uhlmann et al., 1999, 2000). In meiotic cohesin of both fission and budding yeast, Rad21 is replaced by its meiotic variant Rec8; this replacement is essential for differential release of the chromosome arm and centromeric cohesion in meiosis I and II (Buonomo et al., 2000; Kitajima et al., 2003; Klein et al., 1999; Watanabe and Nurse, 1999).

Like yeast, the vertebrates analyzed to date have two Rad21/Rec8 proteins, with a similar partition of function (Lee and Orr-Weaver, 2001; Nasmyth, 2001). By contrast, higher plants such as Arabidopsis and rice (Bai et al., 1999; da Costa-Nunes et al., 2006; Dong et al., 2001; Liu and Makaroff, 2006; Zhang et al., 2006) have four Rad21/Rec8 proteins, only one of which (Syn1/DIF1 in Arabidopsis, OsRad21-4 in rice) (Bai et al., 1999; Bhatt et al., 1999; Cai et al., 2003; Zhang et al., 2006) has been identified as essential for meiosis. Identifying the biological function of the other three proteins is important for further understanding why higher plants contain four Rad21/Rec8 proteins.

Here we have characterized the function of OsRad21-3 by phylogenetic, gene expression, protein immunolocalization and RNAi-mediated reverse genetic analyses. Our results showed that OsRad21-3 is an orthologue of yeast Rad21. The *OsRAD21-3* transcript is preferentially present in flowers, and displays timing of expression that is different from that of the other three *OsRAD21* genes (Zhang et al., 2004, 2006, data not shown). Its expression in flowers persists until the mature pollen stage. Use of RNA interference to knock-down *OsRAD21-3* expression led to arrested mitosis and aberrant chromosome behaviors in developing pollen. These results indicate that OsRad21-3 protein plays a role in pollen development.

Results

Characteristics of OsRad21-3

Our previous analyses predicted that the rice genome encodes four Rad21/Rec8-like proteins – OsRad21-1, OsRad21-2, OsRad21-3 and OsRad21-4 (Zhang et al., 2006). The full-length OsRAD21-3 cDNA (AK101268) of 2856 bp is capable of encoding a polypeptide of 728 amino acids with a calculated molecular mass of 80.2 kDa. A BLASTN search of the TIGR rice genomic database gave a hit for the full-length cDNA in chromosome 8 only (Figure S1a), which indicates that the gene is a single-copy gene. OsRAD21-3 cDNA showed no obvious similarity with any of the other three OsRAD21 cDNAs (Zhang et al., 2006).

Like OsRad21-1 and OsRad21-4 (Zhang et al., 2004, 2006) and other known Rad21/Rec8 proteins from other species (Zhang et al., 2004), OsRad21-3 consists of the complete Pfam04825 and Pfam04824 domains in its N-terminus (amino acids 1–110) and C-terminus (amino acids 669–723), respectively, and a long linker region between them. The middle linker sequence shows high variance in sequence and length compared with other Rad21/Rec8 proteins, and contains a potential bipartite nuclear localization signal (amino acids 378–394), a separase recognition site (amino acids 154–164) and two PEST motifs (amino acids 229–263 and 490–503). These motifs are functionally conserved in the known Rad21/Rec8 proteins (Nasmyth, 2001; Zhang et al., 2004). Consistent with these features, OsRad21-3 showed nucleus localization in a transient experiment with onion epidermic cells (Figure S1b).

OsRad21-3 displays only low similarity with the other three OsRad21s in rice (approximately 22% overall amino acid identity), and the similarity is limited mainly to the domain-containing N- and C-terminal regions. A comparison of sequence similarity between OsRad21-3 and the other three OsRad21s or Rad21/Rec8 proteins from other species revealed that OsRad21-3 was more similar to Arabidopsis Syn3 (also called AtRad21.2) than to the others. In addition, phylogenetic analysis based on Clustal W alignments of N-terminal Pfam04825 domain regions, which are highly conserved in all known Rad21/Rec8 proteins (Zhang et al., 2004), revealed that OsRad21-3 tended to form a group with known members of the Rad21 subfamily from

yeast (Michaelis *et al.*, 1997), *Drosophila* (Warren *et al.*, 2000), *Caenorhabditis elegans* (Pasierbek *et al.*, 2001), mice and humans (McKay *et al.*, 1996). Together, these results suggest that OsRad21-3 is a member of the Rad21 subfamily.

OsRAD21-3 *is expressed preferentially in flowers*

Semi-quantitative RT-PCR revealed that *OsRAD21-3* expressed preferentially in flowers, and weakly in leaves, buds and roots (Figure 1a). Furthermore, immunoblot analysis with antibody to OsRad21-3 revealed that the protein was most abundant in flowers and barely detectable in leaves, buds and roots (Figure 1b).

To further investigate the expression of *OsRAD21-3* in developing flowers, we collected flowers at various developmental stages based on the length of flowers and young panicles, and performed cytological observations. Flowers that were ≤0.9 mm from panicles of <15 mm were grouped as F1 (stamen and carpel primordia formation stage), flowers of 0.9–2.5 mm in panicles of 15–50 mm as F2 (pollen mother cell formation stage), flowers of 2.5–5 mm in panicles of 50–100 mm as F3 (male meiosis stage), and flowers of 5–7 mm in panicles of >100 mm as F4 (microspore stage). Flowers that were ≥7 mm, with anthers becoming yellow in the panicles remaining before the heading stage, were grouped as F5 (bicellular pollen stage), while those close to

anthesis were grouped as F6 (tricellular pollen stage). Unlike the *OsRAD21-4* transcript, which is at its highest level at the meiosis stage and decreased in level as meiosis proceeds (Zhang *et al.*, 2006), the level of *OsRAD21-3* transcript peaked at F1–F3 and decreased thereafter (Figure 1c). Moreover, immunoblot analysis revealed that the level of OsRad21-3 protein peaked at F2–F4, and then decreased slightly (Figure 1d). The accumulation dynamics of OsRAD21-3 protein in these developing flowers are consistent with pollen development from meiocytes to tricellular pollen.

OsRAD21-3 *is expressed in microspores and pollen grains*

To determine whether *OsRAD21-3* mRNA accumulates in male cells, we performed RNA *in situ* hybridization using DIG-labeled OsRAD21-3 antisense and sense RNA probes. In anthers, signals were detected in pre-meiotic pollen mother cells (PMCs) (Figure S2a), meiotic PMCs (Figure S2b) and microspores (Figure S2c), and were not detected in bicellular and tricellular pollen (data not shown). The signal was present in tapetal cells (Figure S2a–c). Failure to detect a signal in bicellular and tricellular pollen might result from a relatively low level of the transcripts in such pollen. Sense (control) probes did not produce signals in flowers (Figure S2d–f).

To clarify whether the transcript and protein are present in pollen grains, we performed immunoblot experiments using mature and *in vitro*-germinated pollen grains, and revealed that the protein was present in these pollen grains (Figure 2a). Combined with the data above, this result demonstrates that *OsRAD21-3* is expressed in the male cells from PMCs to mature pollen stages.

As the rice genome has four *OsRAD21* genes, we used RT-PCR and immunoblot analysis to examine whether
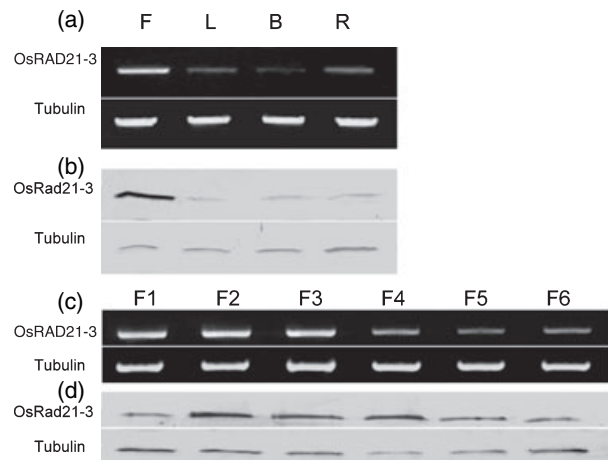

Figure 1. Expression profiles of the *OsRAD21-3* gene.
Expression of *OsRAD21-3* in various tissues (a) and developing flowers (c) was analyzed by semi-quantitative RT-PCR. The PCR products were separated on 1% agarose gels. The amplified rice *tubulin A* mRNA was used as a constitutive control. For Western blot analysis (b, d), total proteins prepared from these materials were subjected to SDS–PAGE, and then immunoblotted using an antibody against OsRad21-3 or against tubulin (control).
(a, b) Patterns of *OsRAD21-3* mRNA (a) and protein (b) accumulation in flowers (F), leaves (L), buds (B) and roots (R).
(c, d) Accumulation profiles of *OsRAD21-3* mRNA (c) and protein (d) in developing flowers at the following stages: stamen and carpel primordial formation (F1), pollen mother cell formation (F2), male meiosis (F3), uninucleate microspore (F4), bicellular pollen (F5) or tricellular pollen (F6).
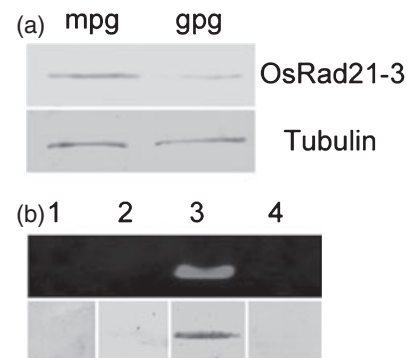

Figure 2. Examination of *OsRAD21-3* transcript and protein in pollen grains.
(a) Western blot detection of OsRad21-3 protein in mature (mpg) and germinated (gpg) pollen grains, with tubulin protein as a constitutive control, using a procedure identical to that described in Figure 1.
(b) RT-PCR analyses of *OsRAD21-1* (1), *OsRAD21-2* (2), *OsRAD21-3* (3) and *OsRAD21-4* (4) transcripts (upper panel), and Western blot results for each corresponding protein (lower panel) in pollen grains.

transcripts and proteins of the other three genes are also present in pollen grains. As seen in Figure 2b, pollen grains contained transcript and protein of *OsRAD21-3* only, not the other genes. Taken together, these results strongly suggest the involvement of *OsRAD21-3* in pollen development.

OsRad21-*3 localizes in mitotic chromosomes*

Considering that the functionally characterized Rad21/Rec8 proteins of various species play roles in chromosome cohesion (Lee and Orr-Weaver, 2001; Nasmyth, 2001; Uhlmann, 2003), we used immunostaining to examine the chromosome localization of OsRad21-3 using an antibody against this protein in root tip cells. The antibody was developed using a non-conserved fragment of OsRad21-3 protein, which has no similarity with any of the other three OsRad21 proteins and did not cross-react with them (Figure S3a). Furthermore, the antibody detected only one band on Western blotting with total proteins prepared from flowers and vegetative tissues (Figure 1b,d, Figure S3b), and the band had an estimated molecular mass similar to the theoretical value for OsRad21-3 (Figure S3b). This result indicates that the antibody specifically recognizes OsRad 21-3. Immunostaining experiments revealed that OsRad21-3

was localized on mitotic chromosomes (Figure 3a–c), but not in other parts of mitotic cells or meiotic cells (data not shown). The labeling signal was detected at interphase (Figure 3a), became strongest at pre-prophase (Figure 3b), decreased sharply at prophase (Figure 3c), and was not detectable at and after metaphase (Figure 3d). This result suggests that a large amount of OsRad21-3 is released during prophase. The selective release feature is similar to that for mitotic cohesin from vertebrates (Waizenegger *et al.*, 2000), which suggests involvement of the protein in chromosome cohesion.

OsRAD21-3i *lines show a decreased seed setting rate*

We addressed the function of *OsRAD21-3* using the RNA interference approach (Wesley *et al.*, 2001). To guarantee the specificity of RNAi, we constructed the OsRAD21-3 RNAi vector pOsRAD21-3i using a 729 bp fragment of OsRAD21-3 cDNA (nt 1278–2006) that shares no similarity to the other three OsRAD21 cDNAs. We obtained 30 independent transformants from rice calli transformed with pOsRAD21-3i. A PCR check for transgene insertion using a primer pair localized in the spacer and inserted cDNA sequences in pOsRAD21-3i revealed the expected fragment of approximately 1 kbp in all 30 T_0 transgenic plants but not in

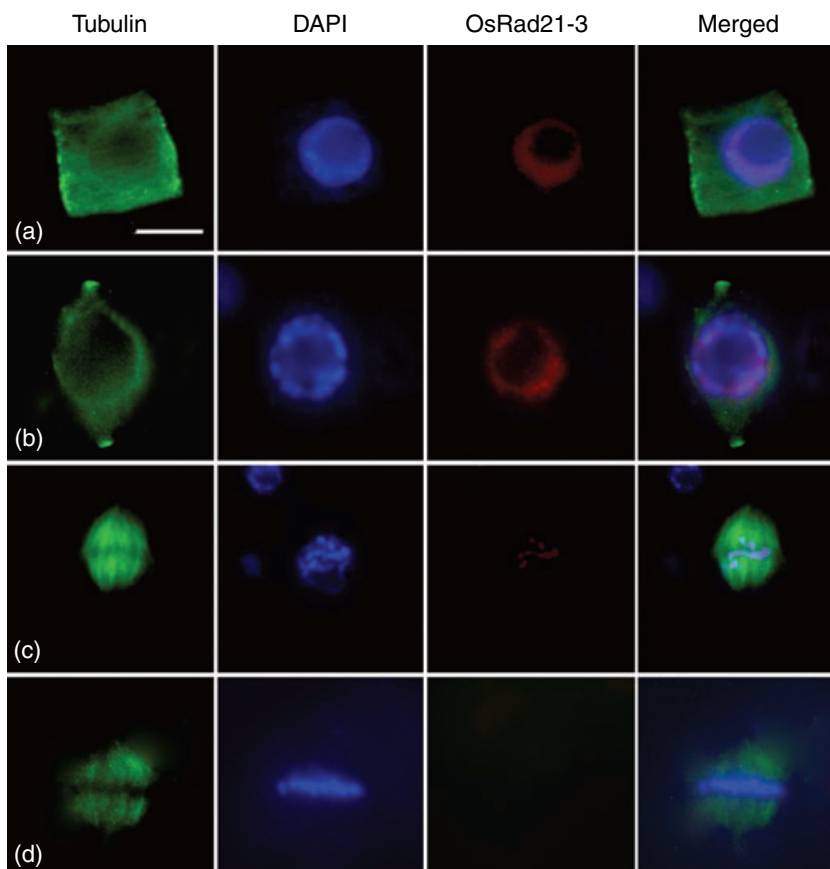| Tubulin	DAPI	OsRad21-3	Merged

Figure 3. Immunofluorescent staining of OsRad21-3 in mitotic chromosomes from root tip cells of wild-type plants.
Nuclear spreads were stained with anti-β-tubulin antibody (green) or with OsRad21-3 antibody (red), and counterstained with DAPI (blue).
(a) Interphase; (b) pre-prophase; (c) prophase; (d) metaphase. Bar in (a) 5 μm, and applies to all images. The results are representative of at least 50 cells for each phase.

wild-type plants. Compared with the wild-type, OsRAD21-3i lines exhibited no detectable abnormalities during vegetative growth. Flowers from these RNAi lines were indistinguishable from those of wild-type. However, in contrast to the wild-type, which had a 90% seed-setting rate, 23 of the 30 lines had a greatly decreased seed-setting rate. Furthermore, we investigated the seed-setting rate of nine of the 23 lines using R_1 plants regenerated from stalks of their T_0 lines. All nine had a low seed-setting rate (10% in one line, 11–46% in six lines and 50–67% in two lines). This finding suggests that *OsRAD21-3* is involved in fertility.

Finally, we examined the insertion copy number of the transgene in the nine lines using Southern blot hybridization, with wild-type plants as a control, and found two insertions in one line, one insertion in the remaining eight lines, and none in wild-type plants. Five RNAi lines (L15, L16, L17, L19 and L23) with a single-copy insertion and representing different sterile phenotypes (Figure 4a) were used for further analysis.

Downregulated OsRad21-3 protein in OsRAD21-3i lines correlates with their sterility

The double-stranded RNA with hairpin structures formed from the transcribed sense–spacer–antisense sequence in RNAi constructs gives rise to small RNAs and ultimately reduces or eliminates the endogenous transcript and protein of a target gene (Hamilton and Baulcombe, 1999). To investigate whether endogenous *OsRAD21-3* transcript and protein were knocked down in the RNAi lines, we examined the levels of endogenous transcript and protein by RT-PCR and Western blot, respectively, in panicles of the L15, L16, L17, L19 and L23 lines, as well as wild-type plants. The endogenous transcript and protein were considerably down-regulated in the five RNAi lines compared with that in the wild-type (Figure 4b,c). We also examined small RNAs specific to OsRAD21-3 by Northern hybridization in the five RNAi lines, and found small RNAs in all five lines but not in the wild-type (data not shown), with the highest level in L16, which is consistent with the most severe down-regulation of the endogenous transcript and protein in the same line. Clearly, down-regulation of both transcript and protein in the RNAi lines is a factor in their sterile phenotypes (Figure 4a–c).

OsRAD21-3i lines show defects in pollen viability

Because pollen is a key regulator of successful fertilization in sexual plants, and because *OsRAD21-3* transcript and protein are present in microspores and pollen grains, we
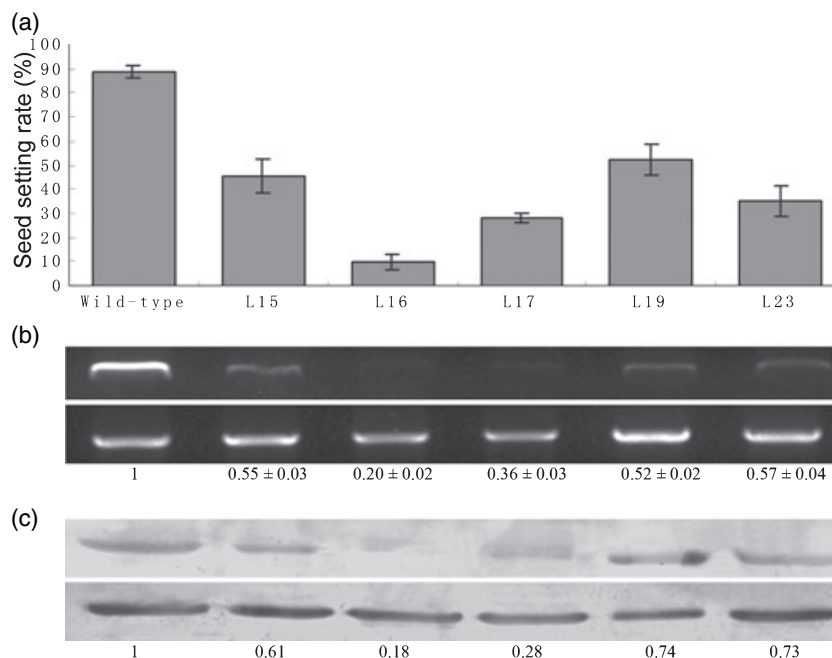

Figure 4. RNAi-mediated down-regulation of *OsRAD21-3* transcript and protein correlates with sterility in OsRAD21-3i lines.
(a) RNAi lines L15, L16, L17, L19 and L23 had severely decreased seed-setting rates compared with wild-type (*t*-test, *P*-value ≤ 0.01).
(b) Endogenous *OsRAD21-3* transcript was greatly down-regulated in the RNAi lines. Semi-quantitative RT-PCR was performed using total RNA extracted from panicles of the RNAi lines and wild-type and the primer pair P1 F/P1R. Top panel: *OsRAD21-3*. Bottom panel: constitutively expressed *tubA*. The quantified levels of *OsRAD21-3* mRNA (data for RNAi lines normalized to that for wild-type) are shown below the panels.
(c) OsRad21-3 protein was deficient in the RNAi lines. The endogenous protein level was detected by Western blotting of total proteins extracted from the panicles of the five RNAi lines and wild-type. Estimated OsRad21-3 protein levels (data for RNAi lines normalized to that for wild-type) are shown below the panels. Top panel: OsRad21-3. Bottom panel: tubulin control.

first examined the viability of mature pollen grains of the five RNAi lines and wild-type plants using I_2-KI and Alexander staining (Alexander, 1969). Starch is preferentially stored in rice pollen and metabolized upon germination to supply a carbon skeleton and energy for the growing pollen tube, and is thus an important indicator of the viability of the pollen (Dai *et al.*, 2006). I_2-KI staining (Figure S4a,b) revealed that more than 95% of wild-type pollen grains ($n = 1263$) were round and had a uniform size, and showed with a dark blue–black reaction, whereas pollen grains from the RNAi lines were variable in size, being smaller or larger than the wild-type, with a greatly decreased number being stained, ranging from 28% ($n = 1671$, in L16) to 75% ($n = 1580$, in L19). Alexander staining (Figure S4c,d) revealed that 95% of wild-type pollen grains ($n = 1230$) were 'viable' (red), whereas approximately 40% ($n = 1660$) of those from L16 appeared 'viable' and the remainder were 'non-viable' (not stained); similar results were observed for the other four lines, in accordance with the I_2-KI assay results.

The staining assays gave only an indirect estimation of pollen viability, so to examine pollen viability directly, we performed *in vitro* pollen germination experiments. Under the assay conditions (Figure S4e,f), 83% of wild-type pollen grains ($n = 644$) germinated, but germination was observed in only 10% of L16 pollen grains ($n = 821$), approximately 30% of L17 pollen grains ($n = 756$), 23% of L23 pollen grains ($n = 766$), and approximately 40% of L15 ($n = 657$) and L19 ($n = 712$) pollen grains (Figure 5). Together, these results indicate that pollen viability is disrupted in the RNAi lines.

Further observations revealed that, although pollen grains from the RNAi lines were variable in size, as compared with the uniform size of wild-type pollen grains, most were round or pear-shaped and only a few were shrunken. Using the method described by Zhang *et al.* (2006), we estimated the pollen amount per anther in these mutants and found no apparent difference compared to the wild-type, which suggests that microsporogenesis might be not disrupted
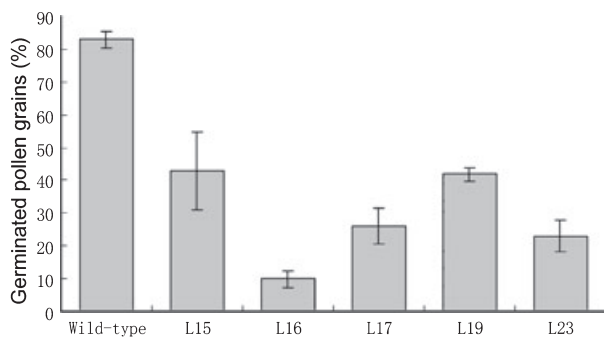
severely in the RNAi lines, and that sterility is mainly derived from abnormal pollen development at the post-meiotic stage.

Male meiosis was not severely disrupted in OsRAD21-3i plants

As the *OsRAD21-3* transcript was detectable in male meiocytes, and to clarify the preceding findings, we observed meiosis behaviors using male meiocytes from the L16, L17 and L23 lines as well as wild-type plants. In wild-type male meiocytes, after synapsis and condensation, homologous chromosomes formed 12 bivalents at diakinesis (Figure 6e) and aligned at the equatorial plate at metaphase I (Figure 6f). The bivalents then underwent reductional division at anaphase I (Figure 6g), generating dyads (Figure 6h). During meiosis II, the two daughter cells divided simultaneously, with two parallel orientations of spindles (Figure 6i), generating tetrads.

In male meiocytes from the RNAi lines (data shown only for L16), meiosis appeared to follow that of the wild-type from leptotene to diplotene (Figure 6a–d). Condensation and synapsis of chromosomes occurred with no noticeable differences compared to the wild-type. At diakinesis, most male meiocytes had 12 recognizable bivalents; only 9% of cells ($n = 80$) had univalents (Figure 6j). The desynapsed homologous chromosomes did not align at the metaphase plate (approximately 7%, $n = 55$) (Figure 6k). As a result, lagging chromosomes appeared at anaphase I (Figure 6l,m) in some male meiocytes (approximately 5%, $n = 60$). During meiosis II, abnormally oriented plates in two daughter cells occurred in <3% of male meiocytes (Figure 6n). Lines L17 and L23 showed less than 5% of male meiocytes with aberrant chromosome behaviors. At the tetrad stage, only a few spores from these RNAi lines appeared to have small nuclei or aberrant size, and the appearance of most (90–95%, $n = 50$) was similar to that of the wild-type. These observations demonstrate that male meiosis was not severely disrupted in the RNAi lines.

OsRAD21-3i lines showed aberrant pollen development at the post-meiotic stage

On the basis of the above results, we examined immature and mature pollen grains from the five RNAi lines as well as from wild-type plants by DAPI staining. After being released from tetrads, wild-type microspores increase in size (Figure 7a,b), with the nucleus migrating to the side opposite to the aperture (Feng *et al.*, 2001; Owen and Makaroff, 1995). This process ends with initiation of asymmetric PMI (Figure 7c), whereby microspores develop into bicellular pollen grains with a dispersed nucleus in the large vegetative cell and a condensed nucleus in the small generative cell (Figure 7d), which then generates two sperm

Figure 5. Pollen viability is disrupted in OsRAD21-3i lines.
The viability of pollen grains (percentage) at the mature pollen stage from wild-type and RNAi plants was examined by *in vitro* germination. The data are the means ± SD of three biological repeats.
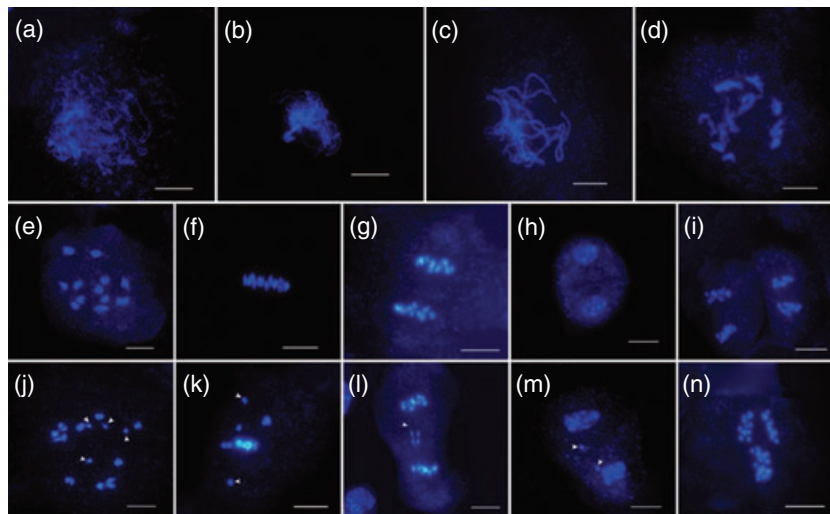
Figure 6. Male meiosis in wild-type and OsRAD21-3i plants.
Nuclear spreads were prepared from fixed anthers from wild-type plants (e–i) and OsRAD21-3i lines (a–d, j–n) and stained with DAPI. Scale bar = 10 μm.
(a–d) Prophase I at leptonema (a), zygonema (b), pachynema (c) and diplonema (d) in the RNAi plants appeared normal.
(e–i) Wild-type male meiosis. (e) Diakinesis, (f) metaphase I, (g) anaphase I, (h) dyads, (i) metaphase II.
(j–n) Male meiocytes from the RNAi lines. (j) Diakinesis, showing univalents (arrowheads); (k) metaphase I and (l) anaphase I, showing lagging chromosomes (arrowheads); (m) early dyads, showing small nuclei (arrowheads); (n) anaphase II, showing the non-parallel plates in two daughter cells.

cells by PMII. Thus, mature pollen grains in rice are tricellular (Figure 7e).

Most microspores from OsRAD21-3i lines (90–95%, $n = 200$) (Figure 7f,g) were indistinguishable from those of the wild-type (Figure 7a,b). However, at the mature pollen stage, at least 90% of pollen grains from the wild-type were tricellular ($n = 1663$) (Figure 7e,m), with about 7% bicellular and 3% aborted (undetectable nucleus and shrunken) (Figure 7m); in contrast, only 15% of mature pollen grains from L16 were tricellular ($n = 2130$) (Figure 7h,m), 71% had an aberrant nucleus appearance (Figure 7i–k,m) and 14% aborted (Figure 7l,m). These defective pollen grains with aberrant nucleus appearance were arrested in the uninucle-ate (Figure 7i) or binucleate (Figure 7j) stage, or had more than three DAPI-stained loci (Figure 7k) and were smaller than wild-type tricellular pollen (Figure 7i–k). A similar situation was found in the other four lines (Figure 7m). The nucleus in the arrested unicellular pollen (Figure 7i) was abnormally condensed. The arrested bicellular pollen grains had a wild-type bicellular pollen-like appearance (Figure 7j versus Figure 7d) that is indicative of the completion of PMI but failure of PMII. All these observations indicate that the OsRad21-3 deficiency in the RNAi lines leads to arrest in mitosis and aberrant chromosome behaviors during pollen development.

The quantified endogenous protein level and the propor-tion of normal tricellular pollen grains in the RNAi lines and wild-type plants were strongly correlated ($r = 0.911$). Together, our results suggest that the OsRAD21-3 deficiency in the mutants resulted in disruption of post-meiotic pollen development.

Discussion

OsRad21-3 is an orthologue of yeast Rad21

Yeast has two members in the Rad21/Rec8 family, Rad21 and its meiotic variant Rec8. Rad21 functions mainly in mitotic cohesion and Rec8 specifically in meiotic cohesion (Klein *et al.*, 1999; Michaelis *et al.*, 1997; Watanabe and Nurse, 1999). This situation is also found in the vertebrates analyzed to date (Lee and Orr-Weaver, 2001; Nasmyth, 2001). By contrast, rice and Arabidopsis have four members of the family, all sharing motif/domain features with the known Rad21/Rec8 proteins from other species (Bai *et al.*, 1999; da Costa-Nunes *et al.*, 2006; Zhang *et al.*, 2004, 2006). However, only one (OsRad21-4 in rice, Zhang *et al.*, 2006; Syn1 in Arabidopsis, Bai *et al.*, 1999) has been identified as essential for meiosis.

In Arabidopsis, the three other *RAD21*-like genes show overlapping profiles of expression in a wide variety of tissues (da Costa-Nunes *et al.*, 2006). The function of *SYN3/AtRAD21.2* remains unknown, but single or double mutants of the other two genes showed normal growth and devel-opment, which suggests a redundant function of the three genes, at least in normal growth (da Costa-Nunes *et al.*, 2006). Our results show that OsRad21-3 is an orthologue of yeast Rad21. *OsRAD21-3* is expressed in vegetative tissues, albeit at a much lower level than detected in flowers. However, OsRAD21-3i lines did not display obvious defects in vegetative growth. A previous study identified *OsRAD21-1* as another rice orthologue of yeast *RAD21* (Zhang *et al.*, 2004). *OsRAD21-3* shows an expression profile that overlaps
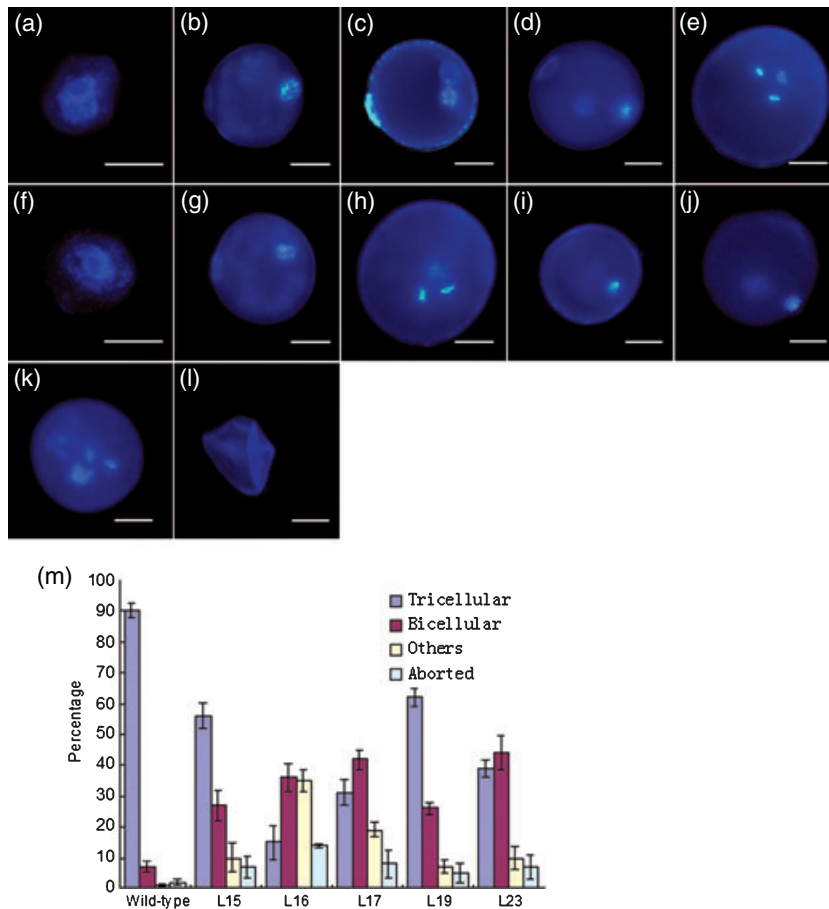
Figure 7. Abnormal pollen development in OsRAD21-3i plants.
Pollen development from uniuncleate microspores to tricellular pollen in wild-type plants (a–e) and RNAi lines (f–l) by DAPI staining. Scale bar = 12.5 μm.
(a–e) Wild-type pollen. (a) Early uninucleate microspore, (b) late uninucleate microspore, (c) early bicellular pollen, (d) mid to late bicellular pollen, (e) mature pollen.
(f, g) Uninucleate microspores from the RNAi lines. (f) Early uninucleate microspore and (g) late uninucleate microspore, showing normal appearance.
(h–l) Pollen grains in the RNAi lines at the mature pollen stage corresponding to the mature pollen phase of wild-type plants. (h) Mature pollen with wild-type tricellular phenotype, (i) arrested unicellular pollen, (j) arrested bicellular pollen, (k) pollen with more than three nuclei, (l) aborted pollen.
(m) Frequencies of normal and aberrant pollen grains at the mature pollen stage in wild-type and RNAi plants. 'Others' include arrested uninucleate microspores and pollen with more than three DAPI-stained loci. The data are the means ± SD of three biological repeats. Compared with the wild-type, RNAi lines showed aberrant pollen development (*t*-test, *P*-values < 0.05).

with that of *OsRAD21-1* in vegetative tissues (Zhang *et al.*, 2004; this paper). Based on these data, *OsRAD21-3* possibly has functional redundancy with *OsRAD21-1* in sporophytic cells.

Possible roles of OsRAD21-3 *in meiosis*

OsRAD21-3i lines displayed aberrant meiotic phenotypes in a low proportion of male meiocytes from late prophase I to meiosis II. Consistent with this finding, the average number of pollen grains per anther in these lines was not decreased significantly compared with the wild-type. By contrast, the Arabidopsis *syn1* mutant and OsRAD21-4 RNAi lines show severe meiotic defects from early prophase I (Bai *et al.*, 1999; Zhang *et al.*, 2006). The defects in early prophase I meiosis in these two mutants and in other plant meiotic

mutants (Li *et al.*, 2005; Nonomura *et al.*, 2004; Pawlowski *et al.*, 2004; Stevens *et al.*, 2004) usually leads to a sharp decrease in male spore number because aberrant spores derived from the defects die early. Based on these observations, *OsRAD21-3* is possibly implicated in meiosis but functions mainly from late prophase I to meiosis II. Alternatively, because OsRAD21-3i lines contained residual OsRad21-3 protein, we cannot rule out the possibility that the residual OsRad21-3 in male meiocytes is sufficient for early meiosis. In fission yeast and mouse, *RAD21* genes have been identified as involved in meiosis, in addition to having important roles in mitosis (Watanabe and Nurse, 1999; Prieto *et al.*, 2002; Prieto *et al.* 2004; Xu *et al.*, 2004).

However, inconsistent with these notions is the fact that the immunostaining experiments described here did not show signals for OsRad21-3 protein in male meiotic

chromosomes. Several studies have suggested that chromosome-bound cohesin protein is undetectable at low levels (Cai *et al.*, 2003; Liu and Makaroff, 2006) and/or that the specific chromatin configuration in some domains blocks access of antibodies against cohesin proteins (Liu and Makaroff, 2006; Tomonaga *et al.*, 2000) for immunostaining. In mammalian cells, well-known mitotic cohesin proteins such as STAG2 and Rad21 were detectable in meiotic chromosomes using antibodies against short peptides but not by antibodies against polypeptides of these proteins (Prieto *et al.*, 2002), which implies that these factors may affect immunostaining detection of OsRad21-3 in meiotic chromosomes. Further experiments using an antibody against short peptides from OsRad21-3 are required to clarify this.

OsRAD21-3 *is required for post-meiotic development of pollen*

In contrast to male meiosis, pollen development at the post-meiotic stage was severely disrupted in OsRAD21-3i lines, which showed arrested uninucleate and binucleate pollen and abnormal chromosome segregation. Together with the expression of *OsRAD21-3* in developing pollen, this result clearly indicates that *OsRAD21-3* is necessary for pollen development. These phenotypes were reminiscent of those found in *Rad21*-deleted vertebrate cells (Sonoda *et al.*, 2001) and the yeast *rad21* mutant (Guacci *et al.*, 1997). In these mutants, aberrant cohesion between sister chromatids contributes to defects in nuclear division and chromosome behaviors (Guacci *et al.*, 1997; Sonoda *et al.*, 2001). Although it difficult to follow the various phases of PMI and PMII (Chen and McCormick, 1996; Durbarry *et al.*, 2005; Howden *et al.*, 1998; Iwakawa *et al.*, 2006), given that the mitotic chromosome localization for OsRad21-3 is similar to that for the Rad21 proteins from yeast and vertebrates (Guacci *et al.*, 1997; Sonoda *et al.*, 2001), we can propose that the role of OsRad21-3 in pollen development results mainly from its involvement in sister chromatid cohesion.

Rad21-containing cohesin coordinates sister chromatid behaviors in cell division by holding them together (Lee and Orr-Weaver, 2001; Nasmyth, 2001); and the cohesin in vertebrates and yeast has been found to have roles in congregating paired sisters into a metaphase plate and in subsequent bipolar attachment of sister kinetochores to a spindle (Uhlmann, 2003). *Rad21*-deleted yeast and vertebrate cells fail to align chromosomes at the metaphase plate and to establish stable attachment of sister kinetochores to a spindle. The failure finally leads to arrested nuclear division by a spindle checkpoint pathway, which functions to guarantee faithful segregation of chromosomes (Sonoda *et al.*, 2001; Toyoda *et al.*, 2002; Uhlmann, 2003). This possibly explains why OsRad21-3 deficiency in RNAi lines causes arrest in pollen mitosis.

Because microspore isolation after meiosis leads to the independent development of individual spores (Twell, 2002), there are two possible explanations for the phenotypic variation observed in the defective spores of OsRAD21-3i plants. The first is that different amounts of residual OsRad21-3 protein are distributed into the spores after meiosis. The presence of a small number of tricellular pollen grains in these RNAi lines indirectly supports this explanation. Alternatively, the *de novo* synthesis of OsRad21-3 in the spores may be disrupted at different levels.

In conclusion, this study shows that, of the four *OsRAD21* genes in the rice genome, only *OsRAD21-3* is expressed in pollen grains and is required for pollen development. Our findings show, in part, why the much-analyzed flowering plants rice and Arabidopsis have four Rad21/Rec8 proteins compared with only two in yeast and metozoans, and give some clues to understanding the functional differentiation of Rad21/Rec8 proteins in evolution.

Experimental procedures

Plant materials and extraction of nucleic acids

Seedlings of cultivar Zhonghua 10 (*Oryza sativa* L. ssp. *japonica*) were planted in soil and raised to maturity. Total RNA extracted various tissues using a Trizol kit (Invitrogen; http://www.invitrogen.com/) was treated with RNase-free DNase I (TaKaRa, http://www.takara.com.cn) to remove residual genomic DNA.

OsRAD21-3 cDNA cloning

A partial cDNA sequence of *OsRAD21-3* was obtained by RT-PCR using gene-specific primers P1 F (5′-ATGTTCTACTCGCACACG-3′) and P1R (5′-CCATAGGCTGCTTCTTGT-3′). This amplified fragment is 2139 bp (accession number AY371048). A full cDNA sequence (accession number AK101268) that has recently been deposited into GenBank is identical to the above sequence, with an additional extension at the 5′ and 3′ ends, and represents the full-length cDNA sequence of *OsRAD21-3*; this sequence was thereafter used in this study.

Expression analysis

Accumulation patterns of *OsRAD21-3* mRNA in various tissues were analyzed by semi-quantitative RT-PCR with primers P1 F and P1R. The transcript of the tubulin *tubA* gene (accession number X91806) was used as a constitutive control (Ding *et al.*, 2002). PCR was performed for 25 cycles. To determine the expression profiles of the gene in various flower cells by *in situ* hybridization, flowers were fixed and further processed as described previously (Ding *et al.*, 2002; Meyerowitz, 1987). DIG-labeled sense and antisense RNAs used for hybridization were synthesized by *in vitro* transcription (Roche, http://www.roche-applied-sciences.com) using a 184 bp cDNA fragment spanning sites 940–1148 of the *OsRAD21-3* cDNA, which shows no similarity to the other three rice *OsRAD21* genes, and was amplified using primers P2 F (5′-CCCTGAACTTAACTTGCC-3′) and P2R (5′-AGATAATCCACCTTGACC-3′).

Polyclonal antibody production and Western blotting

A 729 bp fragment of *OsRAD21-3* cDNA corresponding to amino acids 382–623, which shares no similarity to the other three *OsRad21* genes, was amplified with primers P3 F (5′-TAGGATCCATTGATGGCGGTGAACTAC-3′, added *Bam*HI site underlined) and P3R (5′-TAGTCGACGAATCTCGGGCAAATCTC-3′, added *Sal*I site underlined), cloned into pET-28a(+) (Novagen, http://www.emdbiosciences.com), and confirmed by sequencing. *Escherichia coli* DH5α cells carrying the resulting plasmid were cultured to generate the polypeptide fragment of the OsRad21-3 protein. The recombinant protein purified by Ni^{2+} affinity chromatography (Qiagen; www.qiagen.com/) was used for generation of a polyclonal rabbit antibody against OsRad21-3.

Total protein preparation from various tissues and Western blot detection of OsRad21-3 were conducted according to the methods described by Zhang *et al.* (2006). The primary antibody used was that against OsRad21-3 (1:4000 dilution) or tubulin (1:5000 dilution, Sigma; http://www.sigmaaldrich.com/). The antigen–protein complex was detected using goat anti-rabbit IgG-conjugated alkaline phosphatase.

Subcellular localization and fluorescence immunostaining

The whole ORF of OsRAD21-3 amplified using primers P4 F (5′-TATGGATCCGATGTTCTACTCGCACAC-3′) and P4R (5′-AGTAC-TAGTTTTGGCTCCTGA GAGTGA-3′), with engineered *Bam*HI and *Spe*I enzyme sites at the 5′ and 3′ ends, respectively, was inserted into pCAMBIA1302 (CAMBIA, http://www.cambia.org), and confirmed by sequencing. The construct 35S::GFP:OsRAD21-3 was bombarded into onion epidermis using the biolistic PDS-1000/He particle delivery system (Bio-Rad; http://www.bio-rad.com/). GFP signals were observed under a microscope with a FITC filter (Zeiss; http://www.zeiss.com/).

Immunolocalization of OsRad21-3 was performed according to the method described by Liu *et al.* (1993). Nuclear spreads were first incubated with primary anti-OsRad21-3 antibody (1:5000 dilution) in a blocking buffer pH 7.4 (5% BSA, 5% goat serum and 0.1% Tween-20 in 1× PBS buffer) at 4°C overnight, and then with TRITC-labeled goat anti-rabbit IgG (Jackson ImmunoResearch Laboratories, http://www.jacksonimmuno.com) (1:100 dilution) or with fluorescein-labeled mouse anti-β-tubulin monoclonal antibody only (Sigma) at room temperature for 2–3 h. Finally, the spreads were counterstained with 4′,6-diamidino-2-phenylindole (DAPI) solution. Signals were detected using a Zeiss fluorescence microscope with two, four and five filters for DAPI, fluorescein and TRITC, respectively. Images obtained by cool CCD were merged using Image Pro-Plus 5.0 software (Media Cybernetics, http://www.mediacy.com).

RNAi vector construction and plant transformation

The OsRAD21-3 RNAi vector was constructed by inserting a 729 bp fragment of *OsRAD21-3* cDNA into pWTC605, an RNAi tool vector derived from pCAMBIA1300 (CAMBIA) (Zhang *et al.*, 2006). First, the cDNA fragment was amplified using primer pairs, either P3 F and P5R (5′-AAGGTACCGAATCTCGGGCAA ATCTC-3′, *Kpn*I site underlined) or P5 F (5′-AAGAGCTCTTGATGGCGGTGAACT AC-3′, *Sac*I site underlined) and P3R (sequences of P3 F and P3R are given above). Finally, the two digested fragments were ligated into pWTC605 in the sense and antisense orientations, respectively.

The resulting RNAi construct, pOsRAD21-3i, was used to transform rice embryonic calli induced from mature embryos of cultivar Zhonghua 10, by the *Agrobacterium tumefaciens* EHA105-mediated method, to generate OsRAD21-3 RNAi (OsRAD21-3i) plants, as described by Hiei *et al.* (1994). The regenerated plants from hygromycin-resistant calli were transplanted to soil and grown under standard conditions.

Nuclear and cell spreads

Male meiocyte spreading and DAPI staining were performed according to the method described by Zhang *et al.* (2006). DAPI-stained meiotic chromosomes were observed under a fluorescence microscope (Zeiss Axioskop40, http://www.zeiss.com). For examination of nuclei in microspores and bi/tricellular pollen grains, flowers at the microgametogenesis stage were fixed in ethanol/acetic acid (3:1) solution. Microspores or pollen grains released by squashing the fixed anthers on a slide were stained by DAPI (Park *et al.*, 1998). Each test was repeated three times, and the total number of counted pollen grains was more than 2000 in each case.

Examination of pollen viability and *in vitro* germination

For examination of pollen viability, mature pollen grains were stained in Alexander solution (Alexander, 1969) or 0.1% I_2-KI solution and viewed by light microscopy. The quantified value was the mean of results from three independent experiments.

For *in vitro* germination, mature pollen grains collected at anthesis were immediately transferred into pollen germination medium (0.004% H_3BO_3, 3 mM $Ca(NO_3)_2 \cdot 4 H_2O$, 10% PEG-4000, 20% sucrose, 3 mg l^{-1} VB_1), cultured at room temperature for 10 min, and examined under a light microscope. A pollen grain with a growing pollen tube was considered germinated. The pollen germination rate for each line was calculated using three independent biological samples, and each observation involved examination of at least 600 pollen grains.

Supplementary material

The following supplementary material is available for this article online:
Figure S1. A schematic organization of *OsRAD21-3* gene (a) and subcellular localization of the protein (b).
Figure S2. RNA *in situ* expression analysis of *OsRAD21-3* in developing flowers.
Figure S3. Examination of specificity for the antibody against OsRad21-3.
Figure S4. Pollen viability is disrupted in OsRAD21-3i lines. Viability of pollen grains were examined by I_2-KI Staining (a and b), Alexander staining (c and d) and *in vitro* germination (e and f).
This material is available as part of the online article from http://www.blackwell-synergy.com.

References

Alexander, M.P. (1969) Differential staining of aborted and non-aborted pollen. *Stain Technol.* **44**, 117–122.

Bai, X., Peirsion, B.N., Dong, F., Cai, X. and Makaroff, C.A. (1999) Isolation and characterization of *SYN1*, a *RAD21*-like gene essential for meiosis in Arabidopsis. *Plant Cell*, **11**, 417–430.

Bhatt, A.M., Lister, C., Page, T., Fransz, P., Findlay, K., Jones, G.H., Dickinson, H.G. and Dean, C. (1999) The *DIF1* gene of Arabidopsis is required for meiotic chromosome segregation and belongs to the REC8/RAD21 cohesin gene family. *Plant J.* **19**, 463–472.

Buonomo, S.B.C., Clyne, R.K., Fuchs, J., Loidl, J., Uhlmann, F. and Nasmyth, K. (2000) Disjunction of homologous chromosomes in meiosis I depends on proteolytic cleavage of the meiotic cohesion Rec8 by separin. *Cell*, **103**, 387–398.

Cai, X., Dong, F., Edelmann, R.E. and Makaroff, C.A. (2003) The Arabidopsis SYN1 cohesin protein is required for sister chromatid arm cohesion and homologous chromosome pairing. *J. Cell Sci.* **116**, 2999–3007.

Chen, Y.C.S. and McCormick, S. (1996) *sidecar pollen*, an *Arabidopsis thaliana* male gametophytic mutant with aberrant cell divisions during pollen development. *Development*, **122**, 3243–3253.

da Costa-Nunes, J.A., Bhatt, A.M., O'Shea, S., West, C.E., Bray, C.M., Grossniklaus, U. and Dickinson, H.G. (2006) Characterization of the three *Arabidopsis thaliana* RAD21 cohesins reveals differential responses to ionizing radiation. *J. Exp. Bot.* **57**, 971–983.

Dai, S., Li, L., Chen, T., Chong, K., Xue, Y. and Wang, T. (2006) Proteomic analyses of *Oryza sativa* mature pollen reveal proteins associated with pollen germination and tube growth. *Proteomics*, **6**, 2504–2529.

Ding, Z.J., Wu, X.H. and Wang, T. (2002) The rice tapetum-specific gene RA39 encodes a type I ribosome-inactivating protein. *Sex. Plant Reprod.* **13**, 205–212.

Dong, F., Cai, X. and Makaroff, C.A. (2001) Cloning and characterization of two Arabidopsis genes that belong to the RAD21/REC8 family of chromosome cohesin proteins. *Gene*, **271**, 99–108.

Durbarry, A., Vizir, I. and Twell, D. (2005) Male germ line development in Arabidopsis. Duo pollen mutants reveal gametophytic regulators of generative cell cycle progression. *Plant Physiol.* **137**, 297–307.

Feng, J.H., Lu, Y.Y., Liu, X.D. and Xu, X.B. (2001) Pollen development and its stages in rice (*Oryza sativa* L.). *Chinese J. Rice Sci.* **15**, 21–28.

Guacci, V., Koshland, D. and Strunnikov, A. (1997) A direct link between sister chromatid cohesion and chromosome condensation revealed through the analysis of MCD1 in *S. cerevisiae. Cell*, **91**, 47–57.

Hamilton, A.J. and Baulcombe, D.C. (1999) A species of small antisense RNA in posttranscriptional gene silencing in plants. *Science*, **286**, 950–952.

Hiei, Y., Ohta, S., Komari, T. and Kumashiro, T. (1994) Efficient transformation of rice (*Oryza sativa* L.) mediated by *Agrobacterium* and sequence analysis of the boundaries of the T-DNA. *Plant J.* **6**, 271–282.

Howden, R., Park, S.K., Moore, J.M., Orme, J., Grossniklaus, U. and Twell, D. (1998) Selection of T-DNA-tagged male and female gametophytic mutants by segregation distortion in Arabidopsis. *Genetics*, **149**, 621–631.

Iwakawa, H., Shinmyo, A. and Sekine, M. (2006) Arabidopsis CDKA;1, a cdc2 homologue, controls proliferation of generative cells in male gametogenesis. *Plant J.* **45**, 819–831.

Kitajima, T.S., Miyazaki, Y., Yamamoto, M. and Watanabe, Y. (2003) Rec8 cleavage by separase is required for meiotic nuclear division in fission yeast. *EMBO J.* **22**, 5643–5653.

Klein, F., Mahr, P., Galova, M., Buonomo, S.B.C., Michaelis, C., Nairz, K. and Nasmyth, K. (1999) A central role for cohesions in sister chromatid cohesion, formation of axial elements and recombination during yeast meiosis. *Cell*, **98**, 91–103.

Lalanne, E., Michaelidis, C., Moore, J.M., Gagliano, W., Johnson, A., Patel, R., Howden, R., Vielle-Galzada, J.-P., Grossniklaus, U. and Twell, D. (2004) Analysis of transposon insertion mutants highlights the diversity of mechanisms underlying male progamic development in Arabidopsis. *Genetics*, **167**, 1975–1986.

Lee, J.Y. and Orr-Weaver, T.L. (2001) The molecular basis of sister-chromatid cohesion. *Annu. Rev. Cell Dev. Biol.* **17**, 753–777.

Li, W., Yang, X., Lin, Z., Timofejeva, L., Xiao, R., Makaroff, C.A. and Ma, H. (2005) The AtRAD51C gene is required for normal meiotic chromosome synapsis and double-stranded break repair in Arabidopsis. *Plant Physiol.* **138**, 965–976.

Liu, Z. and Makaroff, C.A. (2006) Arabidopsis separase AESP is essential for embryo development and the release of cohesin during meiosis. *Plant Cell*, **18**, 1213–1225.

Liu, B., Marc, J., Joshi, H.C. and Palevitz, B.A. (1993) A gamma-tubulin-related protein associated with the microtubule arrays of higher plants in a cell cycle-dependent manner. *J. Cell Sci.* **104**, 1217–1228.

Ma, H. (2005) Molecular genetic analyses of microsporogenesis and microgametogenesis in flowering plants. *Annu. Rev. Plant Biol.* **56**, 393–434.

McCormick, S. (2004) Control of male gametophyte development. *Plant Cell*, **16**, S142–S153.

McKay, M.J., Troelstra, C., van der Spek, P., Kanaar, R., Smit, B., Hagemeijer, A., Bootsma, D. and Hoeijmakers, H.J. (1996) Sequence conservation of the *rad21 Schizosaccharomyces pombe* DNA double-strand break repair gene in human and mouse. *Genomics*, **36**, 305–315.

Meyerowitz, E.M. (1987) In situ hybridization to RNA in plant tissues. *Plant Mol. Biol. Rep.* **5**, 242–250.

Michaelis, C., Ciosk, R. and Nasmysh, K. (1997) Cohesions: chromosomal proteins that prevent premature separation of sister chromatids. *Cell*, **91**, 35–45.

Nasmyth, K. (2001) Disseminating the genome: joining, resolving and separating sister chromatids during mitosis and meiosis. *Annu. Rev. Genet.* **35**, 673–745.

Nonomura, K., Nakano, M., Fukuda, T., Eiguchi, M., Miyao, A., Hirochika, H. and Kurata, N. (2004) The novel gene *homologous pairing aberration in rice meiosis 1* of rice encodes a putative coiled-coil protein required for homologous pairing in meiosis. *Plant Cell*, **16**, 1008–1020.

Owen, H.A. and Makaroff, C.A. (1995) Ultrastructure of microsporogenesis and microgametogenesis in *Arabidopsis thaliana* (L.) Heynh. ecotype Wassilewskija (*Brassicaceae*). *Protoplasma*, **185**, 7–21.

Park, S.K., Howdenm, R. and Twell, D. (1998) The *Arabidopsis thaliana* gametophytic mutation *gemini pollen1* disrupts microspore polarity, division asymmetry and pollen cell fate. *Development*, **125**, 3789–3799.

Pasierbek, P., Jantsch, M., Melcher, M., Schleiffer, A., Schweizer, D. and Loidl, J. (2001) A *Caenorhabditis elegans* cohesion protein with functions in meiotic chromosome pairing and disjunction. *Genes Dev.* **15**, 1349–1360.

Pawlowski, W.P., Golubovskaya, I.N., Timofejeva, L., Meeley, R.B., Sheridan, W.F. and Cande, W.Z. (2004) Coordination of meiotic recombination, pairing and synapsis by PHS1. *Science*, **2004**, 89–92.

Prieto, I., Pezzi, N., Buesa, J.M. *et al.* (2002) STAG2 and Rad21 mammalian mitotic cohesins are implicated in meiosis. *EMBO Rep.* **3**, 543–550.

Prieto, I., Tease, C., Pezzi, N. *et al.* (2004) Cohesin component dynamics during meiotic prophase I in mammalian oocytes. *Chromosome Res*, **12**, 197–213.

Sonoda, E., Matsusaka, T., Morrison, C. *et al.* (2001) Scc1/Rad21/Mcd1 is required for sister chromatid cohesion and kinetochore function in vertebrate cells. *Dev. Cell*, **1**, 759–770.

Stevens, R., Grelon, M., Vezon, D., Oh, J., Meyer, P., Perennes, C., Domenichini, S. and Bergounioux, C. (2004) A *CDC45* homolog in Arabidopsis is essential for meiosis, as shown by RNA interference-induced gene silencing. *Plant Cell*, **16**, 99–113.

Tomonaga, T., Nagao, K., Kawasaki, Y. *et al.* (2000) Characterization of fission yeast cohesin: essential anaphase proteolysis of Rad21 phosphorylated in the S phase. *Genes Dev.* **14**, 2757–2770.

Toyoda, Y., Furuya, K., Goshima, G., Nagao, K., Takahashi, K. and Yanagida, M. (2002) Requirement of chromatid cohesion proteins Rad21/Scc1 and Mis4/Scc2 for normal spindle–kinetochore interaction in fission yeast. *Curr. Biol.* **12**, 347–358.

Twell, D. (2002) Pollen developmental biology. In *Plant Reproduction*, **Vol. 6** (Roberts, J.A., ed.). Sheffield: Sheffield Academic Press, pp. 86–153.

Uhlmann, F. (2003) Chromosome cohesion and separation: from men and molecules. *Curr. Biol.* **13**, R104–R114.

Uhlmann, F., Lottspeich, F. and Nasmyth, K. (1999) Sister chromatid separation at anaphase onset is promoted by cleavage of the cohesin subunit Scc1p. *Nature*, **400**, 37–42.

Uhlmann, F., Wernic, D. and Poupart, M.A. (2000) Cleavage of cohesin by the CD clan protease separin triggers anaphase in yeast. *Cell*, **103**, 375–386.

Waizenegger, I.C., Hauf, S. and Meinke, A. (2000) Two distinct pathways remove mammalian cohesin from chromosome arms in prophase and from centromeres in anaphase. *Cell*, **103**, 399–410.

Warren, W.D., Steffensen, S., Lin, E. *et al.* (2000) The Drosophila RAD21 cohesin persists at the centromere region in mitosis. *Curr. Biol.* **10**, 1463–1466.

Watanabe, Y. and Nurse, P. (1999) Cohesin Rec8 is required for reductional chromosome segregation at meiosis. *Nature*, **400**, 461–464.

Wesley, S.V., Helliwell, C.A., Smith, N.A., Wang, M., Rouse, D.T., Liu, Q., Gooding, P.S., Singh, S.P., Abbott, D. and Stoutjesdijk, P.A. (2001) Construct design for efficient, effective and high-throughput gene silencing in plants. *Plant J.* **27**, 581–590.

Wilson, Z.A. and Yang, C. (2004) Plant gametogenesis: conservation and contrasts in development. *Reproduction* **128**, 483–492.

Xu, H.L., Beasley, M., Verschoor, S., Inselman, A., Handel, M.A. and McKay, M.J. (2004) A new role for the mitotic RAD21/SCC1 cohesin in meiotic chromosome cohesion and segregation in the mouse. *EMBO Rep.* **5**, 378–384.

Zhang, L.R., Tao, J.Y. and Wang, T. (2004) Molecular characterization of *OsRAD21-1*, a rice homologue of yeast *RAD21* essential for mitotic chromosome cohesion. *J. Exp. Bot.* **55**, 1149–1152.

Zhang, L.R., Tao, J.Y., Wang, S.X., Chong, K. and Wang, T. (2006) The rice OsRad21-4, an orthologue of yeast Rec8 protein, is required for efficient meiosis. *Plant Mol. Biol.* **60**, 533–554.